Studies on the Mechanism of the Excitation Step in Peroxyoxalate Chemiluminescence

Cassius V. Stevani,[a] Sandra M. Silva,[a] and Wilhelm J. Baader*[a]

Keywords: Electron transfer / Kinetics / Linear free energy relationships / Luminescence / Peroxyoxalate chemiluminescence

Studies on the mechanism of excited state formation in the peroxyoxalate system have been performed, to corroborate the involvement of the well-known Chemically Initiated Electron Exchange Luminescence (CIEEL) mechanism in the chemi-excitation step of this complex sequence. The singlet quantum yields, extrapolated to infinite activator concentrations (Φ_S^∞), and relative rate constants (k_{CAT}/k_D) of the excitation step have been determined in the presence of several activators for two systems: (i) the complete peroxyoxalate reaction with bis(2,4,6-trichlorophenyl) oxalate; and (ii) the base-catalyzed reaction of 4-chlorophenyl *O*,*O*-hydrogen monoperoxyoxalate, an isolated key intermediate. For five activators commonly used in CIEEL studies (anthracene, 9,10-diphenylanthracene, 2,5-diphenyloxazole, perylene, and rubrene), a linear correlation of $\ln(k_{CAT}/k_D)$ with the voltammetric half-peak oxidation potential ($E_{p/2}$) of the activator was obtained for both systems. The values obtained with 9,10-dicyanoanthracene and 9,10-dimethoxyanthracene did not fit this correlation. A reasonable linear correlation between $\ln(\Phi_S^\infty)$ and $E_{p/2}$ was obtained for all activators. For the commonly used activators, this quantum yield (Φ_S^∞) dependence can be rationalized in terms of the free energy balance of the back electron transfer leading to the formation of the excited state of the activator. However, the Φ_S^∞ values obtained with 9,10-dimethoxyanthracene and 9,10-dicyanoanthracene cannot be explained on the basis of these considerations alone. Thus, although this work presents clear-cut evidence of the operation of the CIEEL mechanism in the peroxyoxalate reaction, the results obtained with less commonly used activators show that several mechanistic details of the CIEEL hypothesis remain to be elucidated.

Introduction

The Chemically Initiated Electron Exchange Luminescence (CIEEL) mechanism was proposed by Schuster,[1] mainly on the basis of studies of isolable cyclic and linear peroxides. The decomposition rates of these peroxides, monitored by the decay of light emission, increased in the presence of polycondensed aromatic hydrocarbons of low oxidation potential and high fluorescence quantum yield (Φ_{FL}): the so-called activators (ACT). The emission intensities were strongly enhanced, compared to those of the uncatalyzed decomposition, and these intensities showed a linear dependence on the activator concentration. Additionally, the rate constants and the emission intensities depended on the oxidation potential of the activator utilized, which was taken as an indication of the occurrence of an electron transfer process in the rate-limiting step. These experimental results, briefly outlined above, led to the formulation of the CIEEL hypothesis, illustrated in Scheme 1 for the case of dimethyl-1,2-dioxetanone. Charge transfer complex formation between the peroxide and the activator, and thermal activation of the O−O bond, is followed by elec-

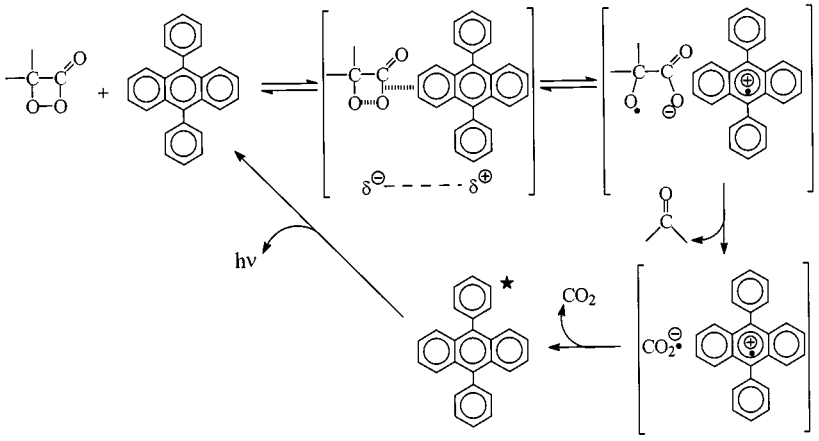

Scheme 1. Simplified CIEEL sequence, demonstrated using dimethyl-1,2-dioxetanone and 9,10-diphenylanthracene

[a] Instituto de Química − Universidade de São Paulo,
C. P. 26077, 05513-970 São Paulo, S. P., Brazil
Fax: (internat.) + 55-11/3815-5579
E-mail: wjbaader@iq.usp.br

  1434−193X/00/1224−4037 $ 17.50+.50/0

tron transfer from the activator to the peroxide, probably simultaneously with O−O bond cleavage.[2] Rupture of the C−C bond and the formation of CO_2 or acetone leaves a pair of radical ions, still in contact inside the solvent cage (radical cation of the activator and radical anion of CO_2 or acetone). The back electron transfer between these two radical ions releases enough energy to promote the activator to its singlet excited state.[2]

Although the CIEEL mechanism adequately explains chemiluminescence catalysis in the decomposition of several peroxides in the presence of certain activators, doubts have been raised about the chemiluminescence quantum yields measured in these systems. The quantum yield for the diphenoyl peroxide/perylene system was shown to be three orders of magnitude lower than the value initially determined.[1,3] Since this is the prototype system for the proposal of the CIEEL mechanism, the validity of the mechanism itself was in question. If the CIEEL mechanism is assumed, then two factors could potentially be responsible for the low quantum efficiency: fast back electron transfer, or diffusion of the radical ions out of the solvent cage.[2]

While there are several known, highly efficient intramolecular CIEEL-like chemiluminescent systems,[4] the peroxyoxalate reaction is the only known system of high chemiluminescence yield[5] that is believed to involve the *intermolecular* CIEEL mechanism. This system consists of the base-catalyzed reaction of hydrogen peroxide with phenolic esters substituted with electron-withdrawing groups in the presence of an activator (Scheme 2).[6] The mechanism of this complex reaction is still not well understood, especially with respect to the excitation step, in which the interaction between the high-energy intermediate and the activator leads to electronic excitation of the latter. This interaction, considered to take place by the CIEEL sequence, cannot be observed kinetically and there is very little clear-cut experimental evidence as to its mechanism.

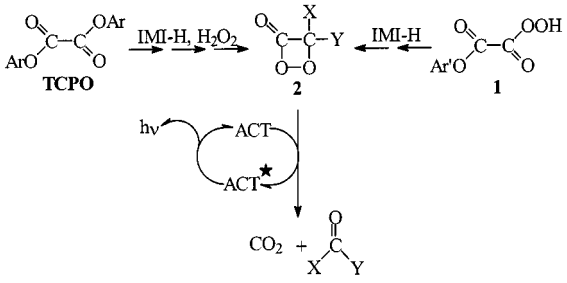

Scheme 2. General scheme for the peroxyoxalate reaction using bis(2,4,6-trichlorophenyl) oxalate (TCPO), and for the reaction of 4-chlorophenyl *O*,*O*-hydrogen monoperoxyoxalate (**1**) with imidazole (Ar: 2,4,6-trichlorophenyl; Ar′: 4-chlorophenyl; IMI-H: imidazole; **2a**: XY: =O; **2b**: X: −OH, Y: −OAr, −OAr′, or -IMI)

Ever since the first reaction of a peroxyoxalate system was reported by Chandross,[7] several peroxides have been postulated as high-energy intermediates. Rauhut et al.[6] proposed 1,2-dioxetanedione as the high-energy intermediate, with the formation of a charge transfer complex between this intermediate and the activator, although there is neither direct experimental nor theoretical evidence for its existence.

Kinetic studies were performed to investigate the mechanism of the reactions prior to the formation of the high-energy intermediate; however, the interaction of this intermediate with the activator in the chemi-excitation step was not observed kinetically.[8−13] More direct experimental evidence was obtained by ^{19}F NMR spectroscopic observations and by the study of the chemiluminescent properties of intermediates involved in the peroxyoxalate sequence.[14−17] Results of kinetic studies on the peracid derivative 4-chlorophenyl *O*,*O*-hydrogen monoperoxyoxalate (**1**) clearly rule out these derivatives as the high-energy intermediates in the peroxyoxalate reaction.[14,15] It should be mentioned, however, that the peroxyoxalate anion of peracid derivatives analogous to **1** has been proposed as the high-energy intermediate in a study of protected peracid derivatives.[17] Since this proposal has yet to be confirmed experimentally, in our opinion, the most probable candidates for the high-energy intermediate structure are 1,2-dioxetanedione (**2a**) and the 1,2-dioxetanone derivative **2b** (Scheme 3). The intermediate **2b** is envisaged as containing the phenolic unit or imidazole as substituent Y, since under certain experimental conditions the reaction proceeds through initial nucleophilic substitution by imidazole.[12,15]

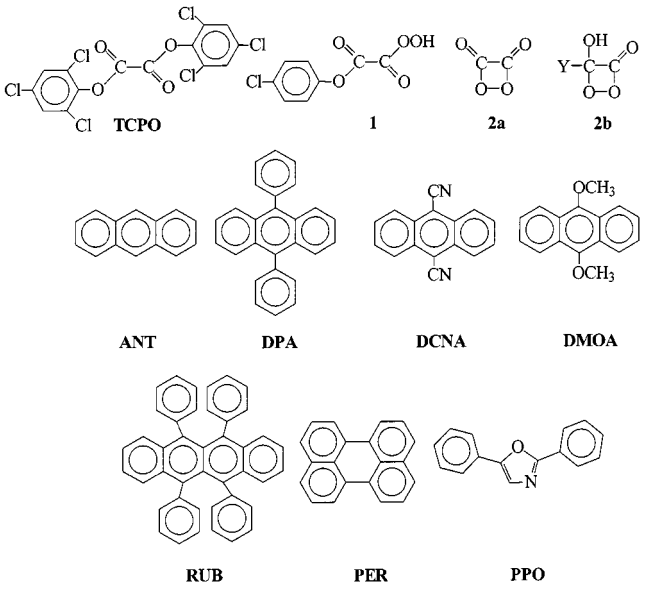

Scheme 3. Structures of TCPO, peracid **1**, high-energy intermediate **2** (Y: −OAr, -IMI), and the activators employed

In this work, we report the singlet quantum yields (Φ_S) of the imidazole-catalyzed reaction of 4-chlorophenyl *O*,*O*-hydrogen monoperoxyoxalate (**1**) and of bis(2,4,6-trichlorophenyl) oxalate (TCPO) with hydrogen peroxide (Scheme 2) in the presence of rubrene (RUB), perylene (PER), anthracene (ANT), 9,10-diphenylanthracene (DPA), 9,10-dimethoxyanthracene (DMOA), 9,10-dicyanoanthracene (DCNA), and 2,5-diphenyloxazole (PPO) (Scheme 3). TCPO was chosen as the oxalic ester derivative because this reagent is widely utilized in analytical applications,[18] and the peracid **1** was studied since it is the first isolable intermediate from the peroxyoxalate system.[14] Evidence for the occurrence of an electron transfer, or at least a charge trans-

fer, between the high-energy intermediate and the activator has been obtained from the chemiluminescence parameters determined by the relationship $1/\Phi_S$ vs. 1/[activator] for the two systems, in agreement with the CIEEL mechanism. However, in the presence of DCNA and, to a lesser extent, also DMOA − two fluorescents that are not commonly used as activators − significant deviations from the behavior predicted by the CIEEL mechanism are observed.

Results

The Φ_S values for the reaction of **1** with imidazole (IMI-H) (system A) and of TCPO with H_2O_2 and imidazole (system B), both under standard conditions (see Experimental Section), in the presence of different concentrations of the activators RUB, PER, ANT, DPA, DMOA, DCNA, and PPO (Scheme 3), were determined from the integrals of light intensity vs. time curves. The light intensity was calibrated against the luminol standard[19] under instrumental conditions identical to those used for the kinetic experiments (see Experimental Section), and these values were corrected for the fluorescence quantum yields of the activators.[20] The concentration range chosen for each activator was based on its solubility in ethyl acetate and the emission intensity obtained. The correlation between Φ_S and the concentration of the activator is given by Equation (1), deduced directly from the simplified kinetic scheme (Scheme 4).

For each activator, the excitation quantum yield at infinite concentration (Φ_S^∞) was obtained by extrapolation of the double reciprocal relationship $1/\Phi_S$ vs. 1/[activator], according to Equation (1). For all activators, linear plots were obtained as shown in Figure 1 and Figure 2 for systems A and B, respectively.

From the slope of these plots, the ratio k_{CAT}/k_D was calculated [Equation (1)]. This ratio provides relative values for the rate constant (k_{CAT}) of the interaction between the high-energy intermediate and the activator, since the rate constant for the unimolecular decomposition of the high-energy intermediate (k_D) is independent of the nature and concentration of the activator. This approach allows one to obtain relative rate constants (k_{CAT}/k_D) for this interaction; these cannot be measured directly since this reaction step is much faster than the preceding ones.[8−13] The chemilumin-

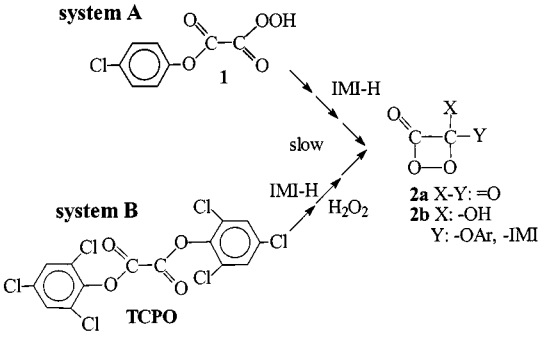

$$2 + ACT \xrightarrow[\Phi_S^\infty]{k_{CAT}} products + ACT^*$$

$$2 \xrightarrow{k_D} products$$

$$ACT^* \xrightarrow[\Phi_{FL}]{k_{FL}} ACT + h\nu$$

$$\Phi_{CL}^\infty = \Phi_S^\infty \Phi_{FL}$$

$$\Phi_S = \Phi_S^\infty \frac{k_{CAT}[ACT]}{k_{CAT}[ACT] + k_D} \Rightarrow$$

$$\Rightarrow \frac{1}{\Phi_S} = \frac{1}{\Phi_S^\infty} + \left(\frac{k_D}{k_{CAT}\Phi_S^\infty}\right)\frac{1}{[ACT]} \quad (1)$$

Scheme 4. Simplified mechanistic scheme for the interaction of the high-energy intermediate with an activator

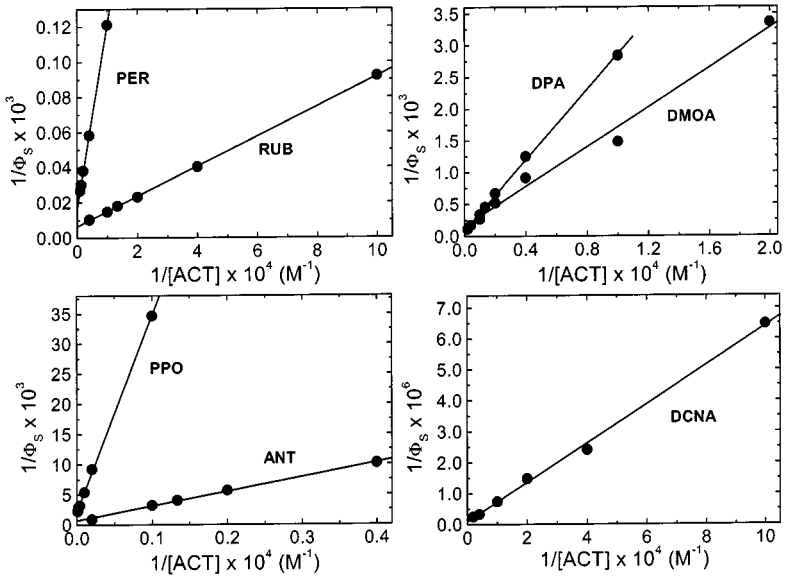

Figure 1. Double reciprocal plot of the singlet quantum yields (Φ_S) vs. the activator concentration for system A

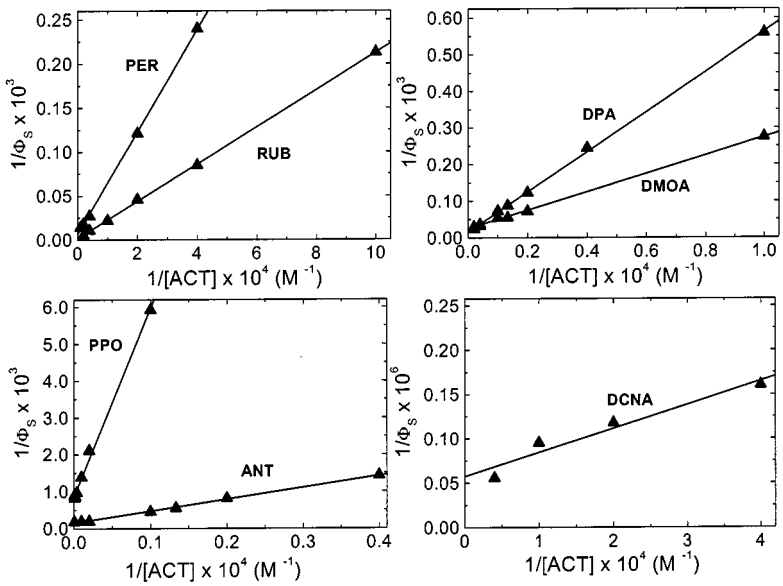

Figure 2. Double reciprocal plot of the singlet quantum yields (Φ_S) vs. the activator concentration for system B

Table 1. Chemiluminescence parameters derived from the reaction of 4-chlorophenyl *O,O*-hydrogen monoperoxyoxalate (system A) or TCPO with H_2O_2 (system B), both catalyzed by imidazole, in the presence of several activators, together with voltammetric half-peak potentials ($E_{p/2}$) and fluorescence quantum yields (Φ_{FL}) of the activators

Activator	$E_{p/2}$ [a] [V vs. SCE]	Φ_{FL} [20]	System A $\Phi_{CL}^{\infty} \times 10^2$ [E mol^{-1}]	System A $\Phi_S^{\infty} \times 10^2$ [E mol^{-1}]	System A $k_{CAT}/k_D \times 10^{-2}$ [mol^{-1} L]	System B $\Phi_{CL}^{\infty} \times 10^2$ [E mol^{-1}]	System B $\Phi_S^{\infty} \times 10^2$ [E mol^{-1}]	System B $k_{CAT}/k_D \times 10^{-2}$ [mol^{-1} L]
RUB	0.61	0.98	16 ± 1	16 ± 1	74 ± 3	67 ± 5	68 ± 5	16 ± 6
PER	0.88	0.87	5.3 ± 2	6.1 ± 0.2	16 ± 1	15 ± 3	17 ± 3	11 ± 3
DMOA	0.90	0.41	0.49 ± 0.08	1.2 ± 0.2	3.9 ± 0.7	1.72 ± 0.04	4.2 ± 0.1	11 ± 4
DPA	1.06	0.95	1.1 ± 0.3	1.2 ± 0.3	3.0 ± 0.7	5.7 ± 0.8	6.0 ± 0.8	3.4 ± 0.8
ANT	1.18	0.27	0.038 ± 0.008	0.14 ± 0.03	2.9 ± 0.8	0.19 ± 0.01	0.69 ± 0.04	5.4 ± 0.8
PPO	1.46	0.70	0.032 ± 0.002	0.046 ± 0.003	0.66 ± 0.06	0.091 ± 0.01	0.13 ± 0.02	0.9 ± 0.3
DCNA	1.80	0.87	(5 ± 3) 10^{-4}	(6 ± 3) 10^{-4}	28 ± 9	(13 ± 3) 10^{-4}	(15 ± 3) 10^{-4}	73 ± 14

[a] In acetonitrile, SCE: saturated calomel electrode.

escence parameters obtained for both systems, together with the voltammetric half-peak potentials – $E_{p/2}$ – for oxidation of the activators are summarized in Table 1. The $E_{p/2}$ potentials were determined experimentally, because reported half-wave potentials obtained under different conditions[20–24] showed discrepancies. For a given electrode process, the relation between the voltammetric half-peak potential and the standard half-wave potential can be a complex one, depending on the mechanism of the process. Thus, standard half-wave electrode potentials of the activator were not determined from the voltammetric experiments because of the lack of knowledge of the mechanisms of the corresponding electrode processes.

The quantum yields for both systems show a similar dependence on the nature of the activator, although the yields are approximately three times lower for the peracid (system A) than for TCPO (system B). This may be caused by impurities in the peracid stock solution. As reported earlier, it was not possible to obtain pure samples of **1**.[14] In contrast, the k_{CAT}/k_D values of the two systems (A and B) proved to be in better agreement, especially with PER, DPA, ANT, and PPO (Table 1). The values for DMOA and DCNA are almost three times higher for system B than for system A, while with RUB, system A gives a value of k_{CAT}/k_D almost 5 times higher (Table 1). However, the general trend in the k_{CAT}/k_D values is the same for systems A and B. Finally, it should be mentioned that none of the activators showed any direct interaction with peracid **1** (no reaction is observed in the absence of imidazole) – a fact that clearly rules out these compounds as high-energy intermediates in the peroxyoxalate reaction, as reported earlier.[14,15]

Furthermore, all the activators utilized proved to be stable under the reaction conditions for at least ten half-lives, as monitored by their absorption spectra. The persistence of the activator is an important fact, especially in the case of DCNA, in which the reproducibility of the kinetic results is somewhat lower than with the other activators; this lower reproducibility is probably due to the very low emission intensities obtained with this activator.

Discussion

The experimental results obtained in this work are discussed in the context of the CIEEL mechanism,[1] shown in Scheme 5 for the peroxyoxalate system. A high-energy

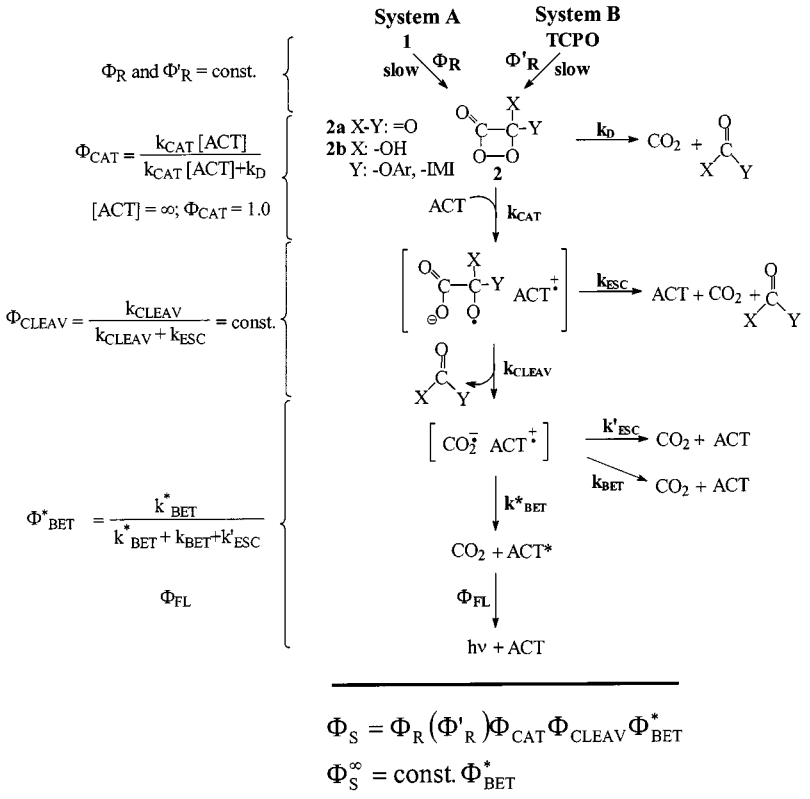

Scheme 5. Mechanistic scheme for excited state formation in the peroxyoxalate reaction, on the basis of the CIEEL mechanism

intermediate is formed from the reaction of the peracid **1** with imidazole (system A) or from the reaction of TCPO with H_2O_2 and imidazole (system B). Although both of the most probable candidates for the high-energy intermediate structure have been considered here (see Introduction), we favor **2a** on the basis of indirect evidence obtained in earlier work.[12,15] However, it should be emphasized that the aim of this work is neither to identify the structure of the high-energy intermediate, nor to establish the occurrence of a common intermediate in systems A and B. The conclusions obtained from our experimental results are the same independently of whether **2a** or **2b** (containing the 2,4,6-trichlorophenyl, 4-chlorophenyl, or the imidazole group as substituent) is the high-energy intermediate. Even if this intermediate were a deprotonated peracid derivative, this would not affect the interpretation of our results.

Rate-limiting electron transfer from the activator to the high-energy intermediate **2** (k_{CAT}), which should be accompanied by the cleavage of the peroxide bond[25] [in competition with dark decomposition of **2** (k_D)], results in a pair of radical ions. The electron transfer may be preceded by charge-transfer complex formation, as postulated earlier,[6] though no experimental evidence for its formation or stability is so far available. Fast carbon−carbon bond cleavage of the radical anion, inside the solvent cage (k_{cleav}), leads to the formation of the radical anion of CO_2, still paired with the activator radical cation. In the case of **2b** acting as the high-energy intermediate, the radical anion of a carbonic acid ester may be involved in the ion pair. However, since CO_2 should have a lower reduction potential,[26] it is more likely to be formed as the radical anion component. The carbon dioxide radical anion and the cation radical of the activator, still inside the solvent cage, undergo rapid, exergonic back electron transfer (BET), leading to carbon dioxide and the activator in either its excited singlet state (k_{BET}*) or ground state (k_{BET}). Of course, cage escape of radical ions (k_{esc} and k'_{esc}) will lead to formation of ground state products. Adam et al. have recently obtained clear-cut experimental evidence for the occurrence of an intermolecular back electron transfer in the excitation step of the triggered decomposition of spiroadamantyl-substituted 1,2-dioxetanes containing protected phenolate ions − from the solvent-cage effect on the singlet chemi-excitation yields obtained in this reaction.[27]

The yields of each reaction step, relative to the pathway leading to excited state formation, can be obtained from the kinetic scheme, and the singlet quantum yield can be expressed as a function of the yields of each individual step (Scheme 5).

A correlation between the values of $\ln(k_{CAT}/k_D)$ and $E_{p/2}$ of the activator (Figure 3) is expected from the CIEEL scheme (Scheme 5), since rate-limiting electron transfer between the activator and the high-energy intermediate **2** is proposed as the first step of the mechanism. Therefore, the k_{CAT}/k_D values should correlate with the oxidation potentials of the activators, because the reduction potential of **2** remains unchanged [Equation (2)].[1] This correlation is only observed if the activator DCNA is excluded (Figure 3). The electron transfer coefficient (α), obtained according to Equation (2), provides an empirical indicator of the sensit-

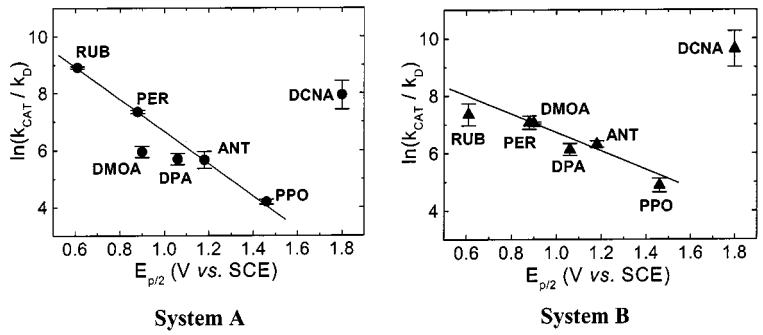

Figure 3. Correlation of the chemiluminescence parameter k_{CAT}/k_D with the voltammetric half-peak potential of the activator ($E_{p/2}$) for system A ($R = 0.99$, without DMOA and DCNA) and system B ($R = 0.98$, without DMOA and DCNA)

ivity of the k_{CAT} value to changes in the oxidation potential of the activator. This parameter is presumably related to the extent of electron transfer in the transition state and, since peroxide bond cleavage should occur simultaneously with electron transfer, α is also a measure of the extent of O−O bond cleavage in the transition state.[25]

$$k_{CAT} = A\exp\left[\frac{-\alpha}{RT}\left(E_{ox} - E_{red} - \frac{e^2}{R_o\varepsilon}\right)\right]$$

$$\ln(k_{CAT}) = \ln A + \alpha B - \left(\frac{\alpha}{RT}\right)E_{ox} \qquad (2)$$

$$\text{Where: } B = \frac{e^2}{R_o\varepsilon RT} + \frac{E_{red}}{RT}$$

α: electron transfer coefficient; R: gas constant; T: temperature; E_{ox}: activator oxidation potential; E_{red}: high-energy intermediate reduction potential, which is constant; e: electron charge; R_o: distance between radical ions in charge transfer complex; ε: dielectric constant of the solvent

The α values reported here are not true electron transfer coefficients, since voltammetric half-peak potentials were used in the correlations (see above). The apparent α values are rather low for both systems (system A: $\alpha = 0.13 \pm 0.02$; system B: $\alpha = 0.08 \pm 0.01$), and suggest the occurrence of an electron transfer process possessing an early transition state, with little progress made in O−O bond cleavage.[25] The α values reported in the literature for several CIEEL systems, using voltammetric half-wave potentials, are typically in the range of 0.3.[1,21,22,28] The lower apparent α values obtained in our study may be taken as evidence that the electron transfer from the activator to the intermediate **2** is more exergonic than in the case of other CIEEL systems. However, the high k_{CAT}/k_D values obtained for DCNA in both systems are not in agreement with the occurrence of an electron transfer from the activator to the high-energy intermediate in the rate-limiting step of the chemiexcitation sequence.

The observed high k_{CAT}/k_D values for DCNA might be explained by the occurrence of an electron transfer from the high-energy intermediate to the activator, which would also cause O−O bond cleavage in the peroxide. Although there is no precedent for such a process in the literature, a similar suggestion was put forward by Wilson to explain unexpected results with DCNA in the decomposition of tetramethoxy-1,2-dioxetane.[29] In this case, it was suggested that catalysis by DCNA, involving electron transfer in the opposite direction, would also lead to excited state formation, contrary to our observations with the peroxyoxalate system, in which the Φ_S^∞ values for DCNA are extremely low.

The plots of ln Φ_S^∞ vs. the $E_{p/2}$ of the activators are linear for both systems (system A and B, Figure 4) and the values for DMOA and DCNA correlate quite well. However, this correlation is not expected from the CIEEL mechanism (Scheme 5). Since the Φ_S^∞ values were obtained by extrapolation of the double-reciprocal plot to "infinite" activator concentration and have been corrected for the Φ_{FL} of the activator, each high-energy intermediate formed will be intercepted by the activator under these conditions (extrapolation to 1/[activator] = 0). These quantum yields (Φ_S^∞) should therefore be independent of the rate constant for the interaction of the activator with the high-energy intermediate (k_{CAT}), and the quantum yields Φ_S^∞ would not be expected to depend on the activator's oxidation potential (Scheme 5, $\Phi_{CAT} = 1$ for [activator] = ∞, independent of the nature of the activator). However, several steps occur after the initial electron transfer, and the resulting cleavage of the O−O bond (k_{CAT}) and the yields of these steps also influence the quantum yields (Φ_S^∞). Since the cleavage of the radical anion of **2** and the cage escape steps (k_{esc} and k'_{esc}) should not depend on the nature of the activator (Φ_{cleav} = constant), it is presumably the efficiency of the back electron transfer in generating the excited state of the activator (k^*_{BET}) that determines the Φ_S^∞ values (Φ_S^∞ = const. Φ^*_{BET}). Thus, Φ^*_{BET} is determined by the relation between k^*_{BET} and k_{BET}, which depends mainly on the energetics of the process, since the activators used are structurally similar (Scheme 5).

The energy of the transformation to the excited activator is determined only by the energy content of the activator radical cation and the activator singlet energy (E_S), since in all cases the partner species is the same: the carbon dioxide radical anion (Scheme 5). Therefore, one might expect a correlation between E_S of the activators and both Φ^*_{BET} and Φ_S^∞. A dependence of ln Φ_S^∞ on the activator E_S is observed for all of the activators used in this study except DCNA (Figure 5). This correlation is not necessarily expected to be linear, since it is not a linear free energy rela-

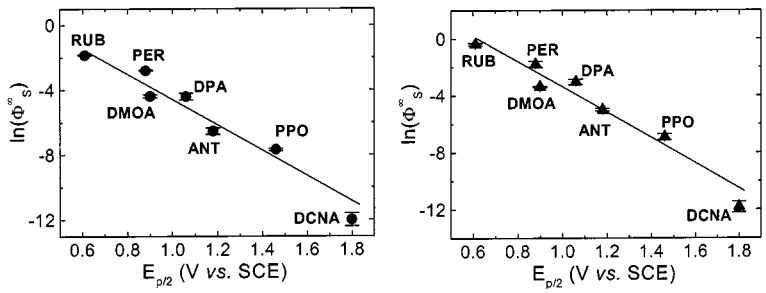

Figure 4. Correlation of the chemiluminescence parameter Φ^{∞}_{S} with the voltammetric half-peak potential of the activators ($E_{p/2}$) for system A and system B

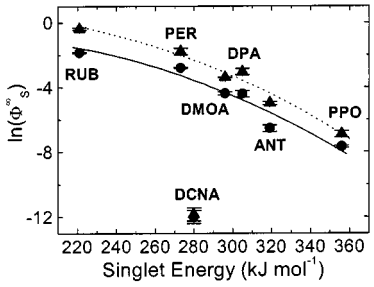

Figure 5. Correlation of the chemiluminescence parameter Φ^{∞}_{S} with the singlet energies of the activators (E_S) for system A and system B (dotted)

tionship. A similar correlation has been observed previously by Turro and Lechtken.[30] The important fact, in the context of our work, is that the values for DCNA also deviate from this correlation.

The free energy change associated with the back electron transfer (BET) from the radical anion of CO_2 to the cation radical of the activators, leading to ground state products (ΔG_{BET}), can be estimated from the half-peak potentials of the activators (Table 1) and the half-wave reduction potential of CO_2 in acetonitrile: $E_{1/2} = -2.2$ V vs. SCE.[31] Obviously, the resulting values are limited by the fact that true thermodynamic electrode potentials were not employed for the activator. However, for purposes of comparison they are still useful. As expected, this free energy change, ΔG_{BET}, is highest for the activators with more positive oxidation potentials (Table 2). In contrast, the free energy balance for BET leading to the singlet excited state (S_1) of the activator (ΔG^*_{BET}), obtained from the singlet energy (E_S) of the activators, shows a higher value for RUB and decreases with more positive oxidation potential for the other activators, with the exceptions of DMOA and, particularly, DCNA (Table 2). If DMOA and DCNA are discounted, the energy balance ΔG^*_{BET} can be utilized to rationalize the Φ^{∞}_{S} values. The BET process will lead to more efficient excited state formation for an activator with higher ΔG^*_{BET} than for one with lower ΔG^*_{BET} (Figure 6 and Figure 7).

Table 2. Free energy balance of the back electron transfer step between the CO_2 radical anion and the activator radical cation

Activator	ΔG_{BET} [a] [kJ mol^{-1}]	E_S (see ref.[20]) [kJ mol^{-1}]	ΔG^*_{BET} [b] [kJ mol^{-1}]
RUB	−318	221	−97
PER	−344	273	−71
DMOA	−346	296	−50
DPA	−362	305	−57
ANT	−373	319	−54
PPO	−400	356	−44
DCNA	−433	280	−153

[a] $\Delta G_{BET} = -F[E_{p/2}\text{ (activator)} - E_{1/2}\text{ (CO}_2\text{)}]$. $E_{1/2}$ (CO_2) = −2.44 V[31] and $E_{p/2}$ (activator) from Table 1, both vs. SHE (standard hydrogen electrode). − [b] $\Delta G^*_{BET} = \Delta G_{BET} + E_S$.

This explanation can also be used to rationalize the correlation observed between ln Φ^{∞}_{S} and the oxidation potentials of the activators. The apparent correlation is due to the fact that the $E_{p/2}$ and E_S values of the commonly utilized activators are related to each other − RUB has a less positive $E_{p/2}$ value and the lowest E_S (Figure 8). The energy released in the BET step, which leads to excited state formation, is determined by the oxidation potential and E_S of the activators. Thanks to the above-mentioned correlation, these values compensate for each other in the cases of the commonly used activators, and so quite similar ΔG^*_{BET} values are obtained (between 44 kJ mol^{-1} for PPO and 97 kJ mol^{-1} for RUB, Table 2 and Figure 7).

The situation for DCNA is completely opposite, as it has the highest ΔG^*_{BET} value and the lowest Φ^{∞}_{S} (Figure 6 and Figure 7). DMOA also does not fit well in the correlation observed with the other activators, although this is not so evident in Figure 6. The ΔG^*_{BET} values for DMOA and ANT are quite similar, but Φ^{∞}_{S} is one order of magnitude lower for ANT than for DMOA in systems A and B. Therefore, the experimental results obtained with these less commonly used activators cannot be rationalized on the basis of the CIEEL mechanism.

Conclusion

The observed linear correlation (Figure 3) of ln (k_{CAT}/k_D) with the oxidation potentials of commonly used activators (RUB, PER, DPA, ANT, PPO) is in agreement with the occurrence of an electron transfer (or at least a charge transfer) in the interaction between a high-energy intermediate (formed in the reaction of peracid **1** or TCPO and H_2O_2 with imidazole) and the activator, as postulated by the CIEEL mechanism. Furthermore, the correlation be-

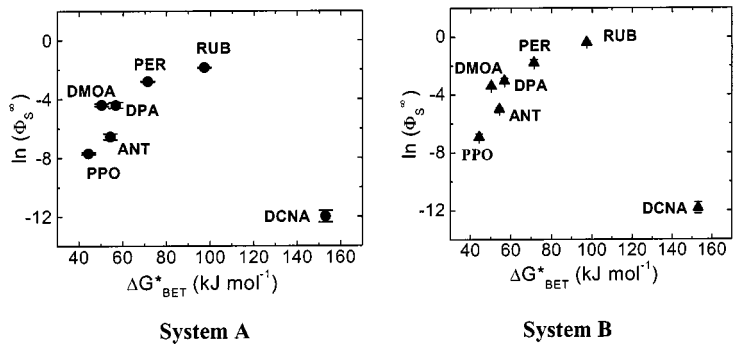

Figure 6. Correlation of the singlet excitation yields (Φ_S^∞) with the free energy change for back electron transfer yielding excited state activators (ΔG^*_{BET})

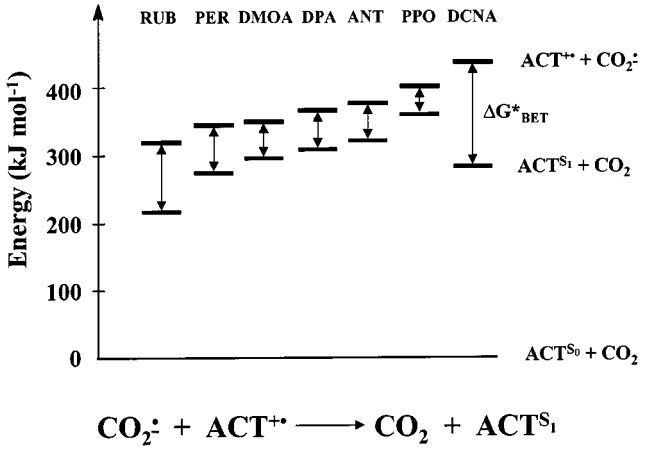

Figure 7. Potential free energy diagram for the back electron transfer between CO_2 radical anion and activator radical cation

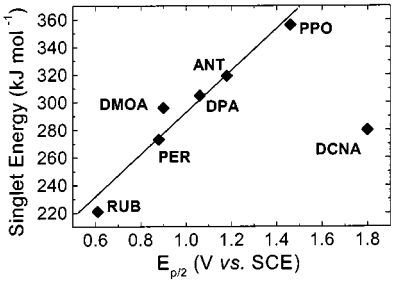

Figure 8. Empirical correlation of the activator singlet energies (E_S) with the voltammetric half-peak potentials of the activators ($E_{p/2}$)

tween ln Φ_S^∞ and $E_{p/2}$ (Figure 4), not expected from the CIEEL mechanism, is due to the parallel behavior of the oxidation potentials and the singlet energies of the activators.

The quantum yields Φ_S^∞ are determined by the energetics of BET from the CO_2 anion radical to the cation radical of the activator, leading to the formation of the excited singlet state (S_1) of the activator (Figure 6 and Figure 7). The free energy change of this step having been calculated on the basis of the CIEEL scheme, this result also contributes to confirm this mechanism. However, data for two less commonly used activators − DMOA and, particularly, DCNA − fail to conform to the CIEEL sequence, implying that details of this mechanism still remain to be clarified.

Experimental Section

Imidazole, rubrene, perylene, anthracene, bis(2,4,6-trichlorophenyl) oxalate, 9,10-diphenylanthracene, 9,10-dimethoxyanthracene, 9,10-dicyanoanthracene (all Aldrich; 99%), and 2,5-diphenyloxazole (Janssen Chimica; 99%) were used as received. 4-Chlorophenyl *O*,*O*-hydrogen monoperoxyoxalate was prepared according to a literature procedure.[14] Ethyl acetate was dried for 1 d over $CaCl_2$, stirred for 30 min in the presence of NaOH (pellets, 40 g L^{-1}) at 0 °C, distilled after filtration, kept for 1 d over 4-Å molecular sieves, carefully distilled (b.p. 77 °C) through a 30-cm Vigreux column under nitrogen and stored over freshly dehydrated 4-Å molecular sieves under nitrogen. − Chemiluminescence measurements were performed with a SPEX-Fluorolog 1681 spectrofluorimeter (slits: 1.0 mm, gratings on mirror position, photomultiplier voltage: 750 V). − The oxidation potentials of the activators were measured using an EG & G Princeton Applied Research model 175 potentiometer-galvanometer with X-Y plotter, scan speed: 100 mV s^{-1}. Absorption measurements were carried out with a Hitachi U-2000 spectrophotometer. − The electrode potentials were obtained by cyclic voltammetry in acetonitrile, using tetraethylammonium perchlorate (0.10 mol L^{-1}) as electrolyte, $Ag/AgNO_3$ as reference electrode, and Pt as the working electrode. The values reported are the anodic voltammetric half-peak potentials ($E_{p/2}$), which are not dependent on the scan rate used and which were converted to saturated calomel electrode (SCE) form to facilitate comparison with other values commonly found elsewhere in the literature. RUB, PER, and DPA exhibited both oxidation and reduction current peaks, while DMOA, ANT, PPO, and DCNA exhibited only an anodic current peak (data not shown).

To determine the chemiluminescence quantum yields for the reaction of 4-chlorophenyl *O*,*O*-hydrogen monoperoxyoxalate or TCPO/H_2O_2 with imidazole in the presence of several activators, the total light emitted under standard reaction conditions {[peracid] = 0.40 mmol L^{-1} (in presence of RUB); 1.0 mmol L^{-1} (in presence of PER, DPA, and PPO); 1.25 mmol L^{-1} (in presence of DMOA); 2.0 mmol L^{-1} (in presence of ANT); 2.25 mmol L^{-1} (in presence of DCNA); [TCPO] = 0.10 mmol L^{-1}, [H_2O_2] = 10 mmol L^{-1}, [IMI-H] = 1.0 mmol L^{-1}} was measured at various activator concentrations.

The experiments with 4-chlorophenyl *O*,*O*-hydrogen monoperoxyoxalate (system A) and TCPO (system B) were carried out in quartz fluorescence or absorption cuvettes (10 × 10 mm, total volume 3.0 mL) at 25 ± 1 °C. The standard procedure for obtaining the kinetic curves with system A was to add, with continuous stirring,

5.0−28 μL of a stock solution of the peracid (240 mmol L^{-1}, determined iodometrically)[32] in ethyl acetate, to a cuvette containing 3.0 mL of the activator (variable concentration) and imidazole (1.0 mmol L^{-1}) in ethyl acetate. In the case of TCPO, the reaction was initiated by simultaneous addition, with continuous stirring, of 50 μL of a TCPO solution (6.0 mmol L^{-1}) and 30 μL of a H_2O_2 solution (1.0 mol L^{-1}), both in ethyl acetate, to a cuvette containing 3.0 mL of activator (variable concentrations) and imidazole solution. Final concentrations: [TCPO] = 0.10 mmol L^{-1}, [H_2O_2] = 10 mmol L^{-1}, [IMI-H] = 1.0 mmol L^{-1}.

The curves of light intensity vs. time were observed over at least three half-lives. With system A, the curves could be fitted to a single exponential function, whereas with system B a double exponential equation had to be used to fit them.[12,15] On the basis of the curve-fitting parameters obtained for both systems (initial intensity for each [activator] and average values of rate constants), the light intensity was extrapolated to zero counts and the integrated areas under the curves (Q_{ACT}) calculated. The total light emitted, obtained initially in arbitrary units (i.e., counts s^{-1}), was converted to Einstein (E) values using the luminol standard[19] [see Equation (3) and Equation (4)]. An average of at least three determinations at each [activator] was used to calculate Φ_S.

$$f_{lum} = \frac{\Phi_{lum} n_{lum}}{Q_{lum}} \quad (3)$$

f_{lum}: luminol calibration factor; Φ_{lum}: luminol chemiluminescence quantum yield; n_{lum}: mols of luminol; Q_{lum}: integral of the light intensity (counts s^{-1}) with luminol

$$\Phi_S = \frac{Q_{ACT} f_{lum} f_{photo}}{n_r \Phi_{FL}} \quad (4)$$

Φ_S: singlet quantum yield; f_{lum}: luminol calibration factor; f_{photo}: photomultiplier wavelength sensitivity factor; n_r: mols of TCPO or peracid **1**; Q_{ACT}: integral of the light intensity (counts s^{-1}) obtained with the activator

Calibration was performed using a modification of the literature procedure.[19] The quantum yield of the luminol reaction (Φ_{lum} = 0.0114 ± 0.0006 E mol^{-1})[33] is independent of the initial luminol concentration over a wide range (10^{-9} to 2×10^{-3} mol L^{-1}).[34] The hydrogen peroxide concentration must be 100 times greater than the luminol concentration,[34] and all solutions (except the stock solution of luminol) must be prepared immediately before the experiment. Stock solutions of luminol [0.10 mmol L^{-1}, in pH 11.6 phosphate buffer (50 mmol L^{-1}), ε_{347} = 7600 M^{-1} cm^{-1}],[33] H_2O_2 (0.30% in deionized water), and hemin (two solutions, with absorbances 0.6 and 0.2 at 414 nm, diluted in the same buffer) were prepared. A cuvette containing 2.8 mL of the luminol solution was placed in the luminometer in the dark, with stirring. To this was rapidly added the H_2O_2 solution (100 μL), followed by the more dilute (absorption 0.2) hemin solution (100 μL). Addition of hemin solution was accompanied by a burst of light, which decayed relatively quickly. As the intensity approached the baseline level (around 2% of the maximum light intensity), the more concentrated (absorbance 0.6) hemin solution (100 μL) was added, and the reaction was monitored until the light intensity reached baseline level. Data acquisition must be started before the addition of the H_2O_2 solution, as the onset of emission is very fast; the total reaction time is around 200 s. After data acquisition, the integral of the light intensity vs. time curve was calculated (Q_{lum}) to derive the quantity of light emitted by the luminol reaction in arbitrary units (i.e., counts s^{-1}). An average of at least ten measurements was used to determine the luminol calibration factor [f_{lum}; Equation (3)].

Correction of the integral light intensities for the wavelength dependence of the detection system was performed in two ways: (i) using the correction factors (f_{photo}) given by the manufacturer at the fluorescence emission maximum of the activator under the experimental conditions, and (ii) recording the fluorescence spectrum of each activator with or without spectral correction by fluorimeter and determining f_{photo} by dividing the integral of the corrected spectrum by that of the uncorrected one. Both methods led to nearly identical results, and for luminol emission the correction factor was approximately 1.0. The excitation quantum yields were finally calculated using Equation (4). Note that Φ_S values are corrected for the fluorescence quantum yield of the activator (Φ_{FL}).

Acknowledgments

We thank Dr. Thérèse Wilson (Harvard University), Prof. Paulo T. A. Sumodjo (University of São Paulo) and Prof. Waldemar Adam (Würzburg University) for helpful discussions, Prof. Frank H. Quina (University of São Paulo) for a critical reading of the manuscript and CNPq, CAPES, FINEP, and FAPESP for financial support. Furthermore, a donation of 60% hydrogen peroxide by Solvay Peróxidos do Brasil Ltda is gratefully acknowledged.

[1] G. B. Schuster, *Acc. Chem. Res.* **1979**, *12*, 366.
[2] T. Wilson, *Photochem. Photobiol.* **1995**, *62*, 601.
[3] L. H. Catalani, T. Wilson, *J. Am. Chem. Soc.* **1989**, *111*, 2633 (see footnote 12 therein).
[4] [4a] A. P. Schaap, T.-S. Chen, R. S. Handley, R. De Silva, B. P. Giri, *Tetrahedron Lett.* **1987**, *28*, 1155. − [4b]L. H. Catalani, A. L. P. Nery, W. J. Baader, *in Chemiluminescence and Bioluminescence* (Eds.: J. W. Hastings, L. J. Kricka, P. E. Stanley), John Wiley & Sons, Chichester, **1996**, p. 23. − [4c]A. L. P. Nery, S. Röpke, L. H. Catalani, W. J. Baader, *Tetrahedron Lett.* **1999**, *40*, 2443. − [4d] A. L. P. Nery, D. Weiß, L. H. Catalani, W. J. Baader, *Tetrahedron* **2000**, *56*, 5317.
[5] C. L. R. Catherall, T. F. Palmer, R. B. Cundall, *J. Biolumin. Chemilumin.* **1989**, *3*, 147.
[6] [6a] M. M. Rauhut, D. Sheehan, R. A. Clarke, A. M. Semsel, *Photochem. Photobiol.* **1965**, *4*, 1097. − [6b] M. M. Rauhut, L. J. Bollyky, B. G. Roberts, M. Loy, R. H. Whitman, A. V. Iannotta, A. M. Semsel, R. A. Clarke, *J. Am. Chem. Soc.* **1967**, *89*, 6515. − [6c] M. M. Rauhut, *Acc. Chem. Res.* **1969**, *2*, 80.
[7] E. A. Chandross, *Tetrahedron Lett.* **1963**, 761.
[8] F. J. Alvarez, N. J. Parekh, B. Matuszewski, R. S. Givens, T. Higuchi, R. L. Schowen, *J. Am. Chem. Soc.* **1986**, *108*, 6435.
[9] M. Orlovic, R. L. Schowen, R. S. Givens, F. Alvarez, B. Matuszewski, N. Parekh, *J. Org. Chem.* **1989**, *54*, 3606.
[10] G. Orosz, *Tetrahedron* **1989**, *45*, 3493.
[11] [11a] H. Neuvonen, *J. Chem. Soc., Perkin Trans. 2* **1987**, 159. − [11b] H. Neuvonen, *J. Chem. Soc., Perkin Trans. 2* **1995**, 945. − [11c] H. Neuvonen, *J. Chem. Soc., Perkin Trans. 2* **1995**, 951.
[12] C. V. Stevani, D. F. Lima, V. G. Toscano, W. J. Baader, *J. Chem. Soc., Perkin Trans. 2* **1996**, 989.
[13] [13a] C. L. R. Catherall, T. F. Palmer, *J. Chem. Soc., Faraday Trans. 2* **1984**, *80*, 823. − [13b] C. L. R. Catherall, T. F. Palmer, *J. Chem. Soc., Faraday Trans. 2* **1984**, *80*, 837.
[14] C. V. Stevani, I. P. de A. Campos, W. J. Baader, *J. Chem. Soc., Perkin Trans. 2* **1996**, 1645.
[15] C. V. Stevani, W. J. Baader, *J. Phys. Org. Chem.* **1997**, *10*, 593.
[16] H. P. Chokshi, M. Barbush, R. G. Carlson, R. S. Givens, T. Kuwana, R. L. Schowen, *Biomed. Chromatog.* **1990**, *4*, 96.
[17] J. R. Hohman, R. S. Givens, R. G. Carlson, G. Orosz, *Tetrahedron Lett.* **1996**, *37*, 8273.
[18] [18a] G. Orosz, R. S. Givens, R. L. Schowen, *Crit. Rev. Anal. Chem.* **1996**, *26*, 1. − [18b] C. V. Stevani, W. J. Baader, *Quím. Nova* **1999**, *22*, 715.

[19] J. Lee, A. S. Wesley, J. F. Ferguson III, H. H. Seliger, *in Bioluminescence in Progress* (Eds.: F. H. Johnson, Y. Haneda), Princeton University Press, Princeton, **1965**, p. 35.
[20] S. L. Murov, I. Carmichael, G. L. Hug, *Handbook of Photochemistry*, 2nd ed., Marcel Dekker, New York, **1993**.
[21] J.-Y. Koo, G. B. Schuster, *J. Am. Chem. Soc.* **1978**, *100*, 4496.
[22] S. P. Schmidt, G. B. Schuster, *J. Am. Chem. Soc.* **1980**, *102*, 306.
[23] V. D. Parker, *J. Am. Chem. Soc.* **1976**, *98*, 98.
[24] A. J. Bard, C. P. Keszthelyi, *J. Electrochem. Soc.* **1973**, *120*, 241.
[25] F. Scandola, V. Balzani, G. B. Schuster, *J. Am. Chem. Soc.* **1981**, *103*, 2519.
[26] J. O'M. Bockris, S. U. M. Khan, *Surface Electrochemistry*, Plenum Press, New York, **1993**.
[27] W. Adam, I. Bronstein, A. V. Trofimov, R. F. Vasil'ev, *J. Am. Chem. Soc.* **1999**, *121*, 958.
[28] [28a] B. G. Dixon, G. B. Schuster, *J. Am. Chem. Soc.* **1979**, *101*, 3116. – [28b] J. P. Smith, A. K. Schrock, G. B. Schuster, *J. Am. Chem. Soc.* **1982**, *104*, 1041. – [28c] M. J. Darmon, G. B. Schuster, *J. Org. Chem.* **1982**, *47*, 4658. – [28d] W. Adam, O. Cueto, *J. Am. Chem. Soc.* **1979**, *101*, 6511.
[29] T. Wilson, *Photochem. Photobiol.* **1979**, *30*, 177.
[30] P. Lechtken, N. J. Turro, *Mol. Photochem.* **1974**, *6*, 95.
[31] M.-M. Chang, T. Saji, A. J. Bard, *J. Am. Chem. Soc.* **1977**, *99*, 5399.
[32] M. L. Cotton, H. B. Dunford, *Can. J. Chem.* **1973**, *5*, 582.
[33] J. Lee, H. H. Seliger, *Photochem. Photobiol.* **1965**, *4*, 1015.
[34] J. Lee, H. H. Seliger, *Photochem. Photobiol.* **1972**, *15*, 227.

Received June 1, 2000
[O00280]